In vivo and *in silico* comparison analyses of Cry toxin activities toward the sugarcane giant borer

Author for correspondence:
Maria Fatima Grossi-de-Sa,
Email: fatima.grossi@embrapa.br;
Fernando Campos de Assis Fonseca,
Email: fernando.fonseca@ifg.edu.br;
Stéfanie Menezes de Moura, Email:
stefmmoura@gmail.com

Fernando Campos de Assis Fonseca[1,2,3] (iD), José Dijair Antonino[1,2,4,5] (iD),
Stéfanie Menezes de Moura[1,5] (iD), Paolo Lucas Rodrigues-Silva[1,5] (iD),
Leonardo Lima Pepino Macedo[1,5] (iD), José Edílson Gomes Júnior[1,2] (iD),
Isabela Tristan Lourenço-Tessuti[1,5] (iD), Wagner Alexandre Lucena[1,5] (iD),
Carolina Viana Morgante[1,5,6] (iD), Thuanne Pires Ribeiro[1,5] (iD),
Rose Gomes Monnerat[1] (iD), Magali Aparecida Rodrigues[7] (iD),
Iolanda Midea Cuccovia[7] (iD), Maria Cristina Mattar Silva[1,5] (iD)
and Maria Fatima Grossi-de-Sa[1,5,8] (iD)

[1]Embrapa Genetic Resources and Biotechnology, Brasília, DF, Brazil; [2]Biology Cellular Department, Federal University of Brasília (UnB), Brasília, DF, Brazil; [3]Federal Institut of Goias (IFG), Águas Lindas, GO, Brazil; [4]Federal Rural University of Pernambuco (UFRPE), Recife, PE, Brazil; [5]National Institute of Science and Technology, INCT PlantStress Biotech, Embrapa, Brazil; [6]Embrapa Semiarid, Petrolina, PE, Brazil; [7]University of São Paulo (USP-SP), São Paulo, SP, Brazil and [8]Catholic University of Brasília, Brasília, DF, Brazil

Abstract

The sugarcane giant borer, *Telchin licus licus*, is an insect pest that causes significant losses in sugarcane crops and in the sugar-alcohol sector. Chemical and manual control methods are not effective. As an alternative, in the current study, we have screened *Bacillus thuringiensis* (*Bt*) Cry toxins with high toxicity against this insect. Bioassays were conducted to determine the activity of four Cry toxins (Cry1A (a, b, and c) and Cry2Aa) against neonate *T. licus licus* larvae. Notably, the Cry1A family toxins had the lowest LC_{50} values, in which Cry1Ac presented 2.1-fold higher activity than Cry1Aa, 1.7-fold larger than Cry1Ab, and 9.7-fold larger than Cry2Aa toxins. *In silico* analyses were performed as a perspective to understand putative interactions between *T. licus licus* receptors and Cry1A toxins. The molecular dynamics and docking analyses for three putative aminopeptidase N (APN) receptors (TlAPN1, TlAPN3, and TlAPN4) revealed evidence for the amino acids that may be involved in the toxin–receptor interactions. Notably, the properties of Cry1Ac point to an interaction site that increases the toxin's affinity for the receptor and likely potentiate toxicity. The interacting amino acid residues predicted for Cry1Ac in this work are probably those shared by the other Cry1A toxins for the same region of APNs. Thus, the presented data extend the existing knowledge of the effects of Cry toxins on *T. licus licus* and should be considered in further development of transgenic sugarcane plants resistant to this major occurring insect pest in sugarcane fields.

Introduction

The sugarcane giant borer, *Telchin licus licus*, Drury 1770 (Lepidoptera: Castiniidae), is one of the most destructive insect pests affecting sugarcane (*Saccharum officinarum*) crops and the sugar-alcohol sector. In northeastern Brazil, this insect pest is responsible for losing about 10–70% of production (Brisceno, 2008). During larval development, which can take up to 110 days, galleries are opened in the sugarcane stalk. This injury reduces the biomass and destroys the meristems of the plants, leading to their death. Furthermore, the infection allows the proliferation of microorganisms that causes sucrose inversion, thereby reducing sugarcane yield. Chemical control of this insect pest is ineffective due to the endophytic behavior of the larvae and pupae (Mendonça *et al.*, 1996). On the other hand, manual control is very limited due to the long time needed to cover wide areas and remove the biological forms. Moreover, in the absence of an effective control method, the insect can spread to noninfested stalks, which significantly increases operating costs (Pinto *et al.*, 2006; Silva-Brandão *et al.*, 2013).

Bacillus thuringiensis (*Bt*) is a Gram-positive bacterium that produces crystals during the sporulation phase, which contain proteins that are toxic to many insect pests and harmless to plants and vertebrates (Peña *et al.*, 2006). *Bt* toxins act primarily in the insect larval stage of different orders, including Lepidoptera, Coleoptera, and Diptera, by troubling their intestinal epithelium, disrupting the cellular osmotic balance, and leading to insect death by

starvation and septicemia (Vachon *et al.*, 2012). Genes encoding active *Bt* Cry toxins have been introduced into transgenic plants, thereby providing a more effective means of controlling insect pests in agriculture and contributing considerably to reducing the use of synthetic insecticide and, consequently, lowering production costs (Christou *et al.*, 2006; Oliveira *et al.*, 2016; Ribeiro *et al.*, 2017; 2019; ISAAA, 2020). Over 800 *cry* genes have been sequenced and grouped into 78 families of proteins based on amino acid identity (Crickmore, 2022). Among these families, Cry1, Cry2, and Cry9 were found to be highly toxic to lepidopterans (Baranek *et al.*, 2020). In previous research, a Cry1Ia12 mutant tested against neonate larvae of *T. licus licus* showed that the use of Cry toxins could be an efficient method to sugarcane giant borer control (Craveiro *et al.*, 2010). However, a crucial aspect of developing such a technology is screening for the most active toxins against the target pests. Although the Cry1Ia12 mutant exhibited a significant mortality rate against the sugarcane giant borer, there was no information on the activity of other toxins (Craveiro *et al.*, 2010).

Given the paucity of reports detailing receptor-binding sites, research on this topic could facilitate *in vitro* modification of *cry* genes and enable the development of new toxins with higher activity against specific targets. Protein modeling and docking have been used to study changes in toxin–receptor binding of DNA shuffling variants (Craveiro *et al.*, 2010; Lucena *et al.*, 2014; Florez *et al.*, 2018). Knowledge of toxin structure and receptor interaction was used *in silico* to develop a modified Cry1Ac (DI-DII)-ASAL toxin against the *Manduca sexta* aminopeptidase N (APN) protein (MsAPN1) (Tajne *et al.*, 2012). Later, the same toxin was expressed in *Escherichia coli* and tested against other lepidopteran pests, conferring its enhanced activity (Tajne *et al.*, 2013). Two transcriptomes of the sugarcane giant borer have been published, making an important contribution to expanding the genetic information about this insect pest (Fonseca *et al.*, 2015; Noriega *et al.*, 2020). Sequencing data revealed APN genes with high expression in *T. licus licus* midgut tissues (Fonseca *et al.*, 2015), which could act as potential Cry toxin receptors. Investigation of these genes could help develop a biotechnological alternative for pest control, e.g., by modifying specific domains of Cry toxins (Lucena *et al.*, 2014).

Considering the negative impact of the sugarcane giant borer and the scarcity of effective control methods, the search for potential entomotoxic molecules that can be used as biological control agents or the development of sugarcane plants expressing the Cry toxin is essential. In this study, we optimized a bioassay system to test the effects of different recombinant toxins of Cry1 (Cry1Aa, Cry1Ab, and Cry1Ac) and Cry 2 (Cry2Aa) families against *T. licus licus* to contribute to future studies on the effect of Cry toxins in controlling sugarcane giant borer. Furthermore, we applied bioinformatic tools to predict the interactions of the Cry1AC toxin with putative *T. licus licus* receptors to understand and modify specific amino acids to obtain toxins with improved activity.

Materials and methods

Insect rearing

Sugarcane giant borer females were collected from sugarcane fields and placed in boxes for oviposition. Eggs were collected, individually distributed in 96-well plates, and maintained in the laboratory at $26 \pm 2°C$, $70 \pm 10\%$ relative humidity (RH), and a photoperiod of 12:12 (L:D). After hatching, larvae were fed with a liquid artificial diet soaked in previously washed and sterilized absorbent cleaning cloth discs, measuring $0.4\ cm^2$ (Craveiro *et al.*, 2010). The artificial diet contained: 1% yeast extract, 6% sucrose, 0.2% ascorbic acid, 1.1% vitamin mixture, 0.4% Wesson salt mixture, 0.03% cholesterol, 0.3% choline chloride, and water. Larvae were maintained on this diet until its use. The method for insect rearing developed in this work resulted in a national patent (Grossi-de-Sá *et al.*, 2013).

Protein analyses and toxicity bioassay

The acrystalliferous *Bt* strain 407 *cry*⁻, transformed with pHT315 plasmid harboring *cry1Aa*, *cry1Ab*, and *cry2Aa* genes separately (generously provided by Dr Colin Berry of Cardiff University – UK), was used for Cry toxin expression. Cry1Ac was produced from wild-type *Bt* strain HD73. Spore–crystal complexes were suspended in ultrapure water and quantified by the Bradford method (Bradford, 1976). All the transformants were grown for 3 days at 29°C in a nutrient broth sporulation medium (Monnerat *et al.*, 2007). The culture medium was centrifuged at $9000 \times \boldsymbol{g}$ for 20 min at 4°C, and the pellet containing crystals and spores was subsequently recovered and lyophilized. One hundred micrograms of protein were solubilized in loading buffer, incubated at 100°C for 10 min, and subjected to 12% SDS-PAGE.

The *T. licus licus* neonate larvae were exposed to toxins expressed in the acrystalliferous *Bt*, as previously described. For the spore–crystal bioassay, a diagnostic dose of $250\ \mu g\ cm^{-2}$ of suspension was eluted in a liquid artificial diet and employed against the target insect pest. The suspension was diluted in the liquid artificial diet for the expressed toxins to final concentrations of 15.62, 31.25, 62.50, 125, 250, and 500 ng cm⁻². A 50 μl of suspension was soaked into $0.4\ cm^2$ absorbent cleaning cloth discs (80% viscose, 20% polyester). The experimental unit consisted of 12 larvae individually placed in 96-well plates. Six replicates were used for each treatment. An artificial diet without spores or crystal toxins was used in the LC₅₀ bioassays as a negative control, while an artificial diet containing Cry8Ka5 protein, a specific coleopteran toxin (Oliveira *et al.*, 2011), was used in the spore–crystal bioassay. The insects were maintained at $26 \pm 2°C$, $70 \pm 10\%$ RH with a photoperiod of 12:12 (L:D). The mortality rate was calculated according to Abbot's formula (Abbott, 1925). LC₅₀ was calculated by Probit analysis using SPSS package. Percentages of mortality obtained in the bioassays were analyzed using a one-way analysis of variance (ANOVA). Tukey's test ($P < 0.05$) was used to analyze significant differences between treatments.

Solubilization/activation of Cry proteins and osmotic swelling assay

The expressed recombinant toxins were harvested and washed with buffer containing 0.01% Triton X-100, 50 mM NaCl, and 50 mM Tris-HCl, pH 8.5. Crystals were purified by sucrose gradients as reported by Gómez *et al.* (2001, 2002), solubilized at 37°C for 2 h in extraction buffer (50 mM Na_2CO_3, pH 10.5), and then activated with trypsin (1:20 w/w) for 2 h at 37°C. The toxins were also activated for 2 h at 37°C with intestinal homogenate extracted from the insect midgut. PMSF (phenylmethylsulfonyl fluoride) was added at a final concentration of 1 mM to stop proteolysis. For the osmotic swelling assay, brush border membrane vesicles (BBMVs) were purified from midguts isolated from fifth-instar

T. licus licus larvae using modified magnesium precipitation and differential centrifugation procedures (Wolfersberger *et al.*, 1987). The midguts were solubilized in MET buffer (250 mM mannitol, 5 mM EDTA and 17 mM Tris–HCl; pH 7.5) and 1 mM PMSF, according to a 1/10 (w/v) ratio. An equal volume of 24 mM $MgCl_2$ was added to the intestinal homogenate before further steps of the standard protocol were undertaken. Enzymatic assays evaluated the quality of BBMV for alkaline phosphatase and aminopeptidase activity (Rodrigo-Simón *et al.*, 2008).

The membrane permeabilization effects of trypsin-activated Cry toxins were analyzed by an osmotic swelling assay, based on the methodology described by Carroll and Ellar (1993), with some modifications. Vesicles (0.4 mg membrane protein per ml) equilibrated in 10 mM glycine/KOH (pH 9.5) and 1 mg ml^{-1} BSA (bovine serum albumin) were incubated at 25°C for 60 min with 75 pmol mg^{-1} membrane protein of each toxin. The solution was mixed directly in a cuvette with an equal volume of 0.6 M KCl hypertonic solution. Vesicles rapidly shrink in response to this hypertonic shock, causing a sharp rise in scattered light intensity. Depending on their permeability to solutes, the vesicles subsequently recovered some of their original volumes. Scattered light intensity was monitored at 450 nm at an angle of 90° and in an F-7000 FL Spectrophotometer (Hitachi, Chyoda, Tokyo, Japan). The normalized data and percentage volume recovery were analyzed as described by Fortier *et al.* (2005). The final percentage volume recovery was calculated after 5 min. Control values obtained in the absence of toxin were subtracted from those measured in the presence of the toxin. Osmotic swelling experiments were carried out in triplicate. The osmotic swelling assay was performed to analyze the activity of Cry1Aa, Cry1Ab, Cry1Ac, and Cry2Aa toxins. The coleopteran-specific Cry8Ka5 was used as a negative control (Oliveira *et al.*, 2011).

Homology modeling

The amino acid sequence data were submitted to the M4T v.3.0 server (http://manaslu.fiserlab.org/M4T/) to search for the best crystallographic structures to use as templates for modeling and to provide the protein structure alignment file. Next, the amino acid sequences were submitted to three different servers, PSIPRED (http://bioinf.cs.ucl.ac.uk/psipred/), SWISS-MODEL (http://swissmodel.expasy.org/), and PHYRE2 (http://www.sbg.bio.ic.ac.uk/phyre2), to predict the secondary structure of the proteins. This information improved the alignment between the target sequence and the template. After manual curation was performed, the alignment files were used to build 100 model structures using the MODELLER v.9.10 program (Fiser and Sali, 2003). For every structure generated, the program calculated a statistical potential known as DOPE (Discrete Optimized Protein Energy). Models with the lowest DOPE scores represented the most stable protein structures (Shen and Sali, 2006) and were selected for further analysis.

The stereochemical quality of each selected model was analyzed by the PROCHECK program, which is available at the PDBsum database (https://www.ebi.ac.uk/thornton-srv/databases/pdbsum/Generate.html) (Laskowski *et al.*, 1997). The unfavorable regions, if identified in the Ramachandran plot, were realigned and resubmitted to the MODELLER program to generate new models. Only the active forms of the proteins were submitted to homology modeling, as the signal peptide sequences were removed from the APN sequence receptors, and the region corresponding to the processed protoxin of the Cry

proteins was used. The resulting models were validated using a Ramachandran plot.

Molecular dynamics

Molecular dynamics (MD) simulations were performed by the GROMACS v.4.5.3 suite (Berendsen *et al.*, 1995) using the GROMOS 43a1 force field (Van Gunsteren, 1996). The simulation protocol was conducted as specified by de Groot and Grubmüller (2001). For system assembly, the proteins were solvated with SPC (statistical process control) water (Berendsen *et al.*, 1987) in the center of a cubic periodic box. A minimum 1.0 Å-distance simulation box was created such that the protein could be fully immersed in water and rotated freely. Sodium counter ions were added to neutralize the net charge of the system. After a minimization protocol was undertaken using steepest descent and conjugate gradient to eliminate possible clashes and bad contacts, an NVT ensemble (N: fixed number of atoms, V: fixed volume, T: fixed temperature) with restraint forces of 1000 kJ mol^{-1} was performed for 4 ns at 300 K. Moreover, five subsequent equilibration steps in the NPT ensemble (number of particles, pressure, and temperature are constant) were performed at 1 bar with restraint forces of 800 kJ mol^{-1} on heavy atoms, 600 kJ mol^{-1} and 400 kJ mol^{-1} on the main chain, 200 kJ mol^{-1} on the backbone, and 100 kJ mol^{-1} on alpha-carbons totaling 13 ns. Finally, unconstrained runs were performed for 50 ns using an integration step of 2 fs and the LINCS algorithm (Hess *et al.*, 1997). Also, the Particle Mesh Ewald method (Essmann *et al.*, 1995) was applied for Coulombic and Lennard-Jones interactions longer than 1 nm.

Protein docking

Molecular docking was used to identify a way to mimic the formation of heterodimers between Cry toxins and APN receptors from *M. sexta* and *T. licus licus* and to simulate the interaction of the proteins during the first step of the mechanism of action, i.e., the binding of the toxin in its monomeric form to the receptor (Pardo-López *et al.*, 2013). Atomistic coordinates of the models at 50 ns, which were obtained after molecular docking, were submitted to the ClusPro program (Comeau *et al.*, 2004). Models proposed in the literature provide insight into the participation of domain II, loops 2 and 3 of the Cry1A family of toxins in the binding process with APN receptors (Gómez *et al.*, 2006; Pacheco *et al.*, 2009; Arenas *et al.*, 2010). For Cry1Aa, the amino acids that comprise loop 2 are located between positions R367 and E379, while loop 3 consists of amino acids S438–T446. For Cry1Ab and Cry1Ac, loop 2 is represented by residues R368–Q379, and loop 3 consists of the region between R437 and I447 (Herrero *et al.*, 2001). These amino acids were chosen as ligand regions for the toxin models, while no constraints were imposed on the receptor models. Models with the best energetic results that coincide with interaction data described in the literature were selected.

Results

Insect bioassays

Bioassays were conducted to determine the activity of the four recombinant protoxins (Cry1Aa, Cry1Ab, Cry1Ac, and Cry2Aa) against *T. licus licus* neonate larvae and to determine the 50% insect mortality (LC$_{50}$) values (fig. 1). Notably, the Cry1A family toxins were the most effective and had the lowest LC$_{50}$ values
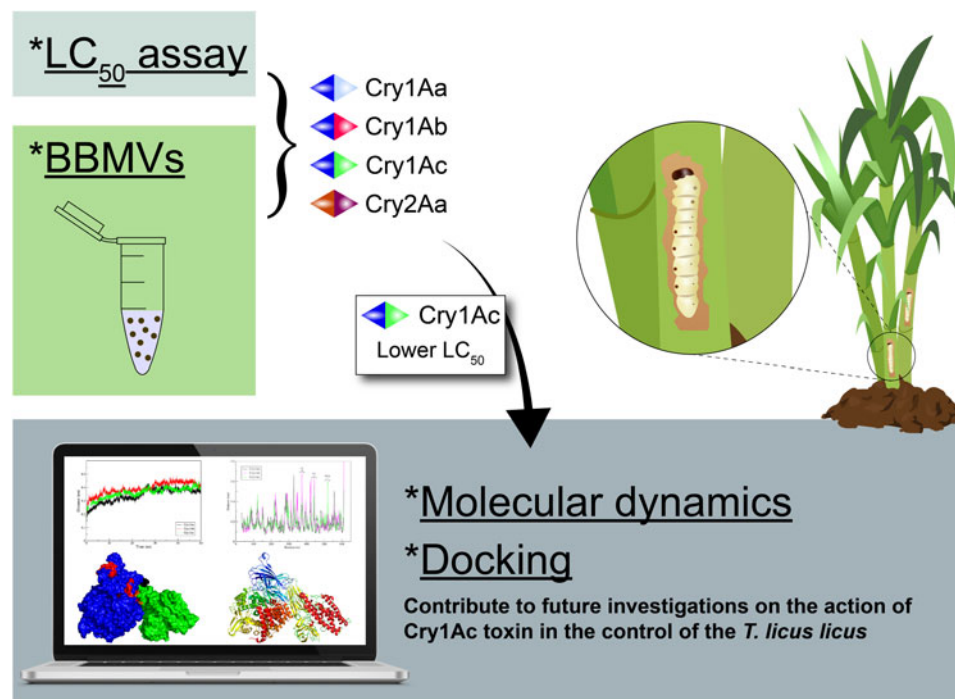
Figure 1. Summary of the experiments performed in this manuscript. *In vivo* analyses determined that Cry1Ac has the lowest LC50 against the sugarcane giant borer (*T. licus licus*) and a new *in silico* computational simulation of toxin/receptor interactions is described.

(table 1). Cry1Ac had the best toxicity, which exhibited 2.1-fold higher activity compared with Cry1Aa, 1.7-fold activity compared with Cry1Ab, and 9.7-fold activity compared with Cry2Aa. The second most active toxin was Cry1Ab, followed by Cry1Aa. The Cry2Aa toxin had a very high LC_{50} (169.2 ng cm^{-2}) compared with the other proteins, with a LC_{50} sixfold higher than the average for the Cry1A family (table 1).

Pore-forming activity analyzes

To evaluate the pore-forming activity of these Cry toxins, osmotic swelling and BBMV assays were performed. Electrophoretic analyses of the suspended spore–crystal complex showed that Cry1Aa, Cry1Ab, and Cry1Ac toxins exhibited a similar protein profile with a distinct band at about 130 kDa, while Cry2Aa exhibited a distinct band at about 60 kDa (fig. S1a). After trypsin activation, all toxins, including those of the Cry1A family and Cry2A, were cleaved into two fragments of approximately 60 and 65 kDa (fig. S1b). However, some differences were evident between the protein profiles in the intestinal homogenate. For instance, activation of Cry1Aa toxin resulted primarily in a

fragment of 55 kDa, whereas Cry1Ab and Cry1Ac were more frequently cleaved into fragments of 60 kDa. In the case of Cry2Aa activation, SDS-PAGE clearly showed that the toxin was overdigested to a fragment of about 50 kDa (fig. S1c).

As a measure of the quality and purity of the BBMV preparation, the leucine APN and alkaline phosphatase enzymatic activities were evaluated in the initial gut homogenate and the last four vesicle suspensions, showing a 7- and 13.5-fold increase in apical membrane enzyme activity, respectively (fig. S2). In the analyses of membrane binding and disruption capacity for these toxins, after treatment of BBMVs with hypertonic solution, a strong turgor followed by a recovery aspect after the addition of trypsin-activated toxins was observed (fig. 2). Notably, the Cry1Ab, Cry1Ac, and Cry2Aa toxins caused significant membrane disruption in *T. licus licus*, with high intensity compared with the effect of a coleopteran-specific Cry8Ka5 toxin (used as a negative control) and also with the lepidopteran-specific Cry1Ia12 toxin (used as a positive control) (fig. 2).

Homology modeling and the molecular dynamics of protein models of toxins and putative receptors

Since the Cry1A family toxins were the most promising, as they presented the lowest LC_{50} values (table 1), we performed *in silico* simulations to predict amino acids that might be involved in the interaction of Cry1A toxins and their putative receptors in *T. licus licus*. To this end, we employed MD and docking for three putative APN receptors (TlAPN1, TlAPN3, and TlAPN4) whose sequences were previously detected in the *T. licus licus* transcriptome (Fonseca *et al.*, 2015; Noriega *et al.*, 2020).

The Cry1Aa structure (PDB:1CIY) was used to model Cry1Ab and Cry1Ac proteins. The human APN structure (PDB:2YD0) was employed to model the three putative APN receptors

Table 1. Median lethal concentration (LC_{50}) of recombinant Cry protoxins against neonate *T. licus licus* larvae

Toxin	LC_{50} (ng cm^{-2})	CI 95% (ng cm^{-2})
Cry1Aa	37.2	21.7–59.6
Cry1Ab	29.7	16.9–48.3
Cry1Ac	17.4	9.16–29.3
Cry2Aa	169.2	106.4–283.5

CI, confidence interval.
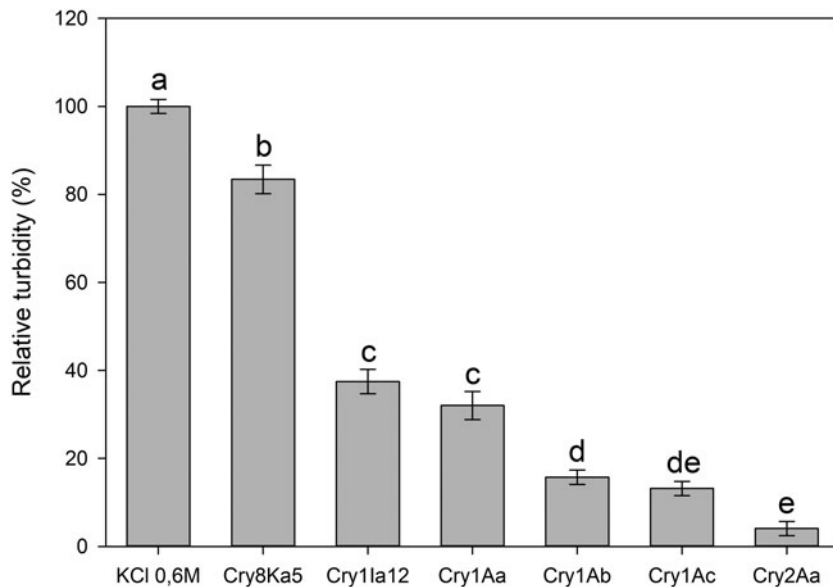
Figure 2. Osmotic swelling assay of trypsin-activated Cry toxins against *T. licus licus* BBMVs. Vesicle permeability was tested in a hyperosmotic solution that keeps them constricted. Membrane disruption is indicated by a reduction in the scattered-light intensity, reflected by the absorbance of the light. Lower absorbance indicates increased membrane disruption. KCl 0.6 M, hypertonic solution; Cry8Ka5 was used as a coleopteran-specific control (used as a negative control); Cry1Ia12 was used as a lepidopteran-specific control (used as a positive control). Bars indicate standard deviation of technical replicates. Letters above bars indicate significant differences at $P < 0.05$ (one-way ANOVA, followed by Tukey's test).

(TlAPN1, TlAPN3, and TlAPN4) (GenBank: MW353178–MW353180) analyzed (Fonseca *et al.*, 2015). In addition, the MsAPN1 was also used for the modeling analyses since it was previously characterized as the Cry1A receptor of *M. sexta* (Masson *et al.*, 1995) (GenBank: Q11001). On average, more than 98% of amino acid residues were located within the favored and allowed regions for all proteins. The resulting protein models were subjected to MD analysis to allow the structures to achieve a low energy state and better conformation.

Systems containing the toxins MsAPN1, TlAPN1, TlAPN3, and TlAPN4, as well as Cry1Aa, Cry1Ab, and Cry1Ac were simulated for 50 ns (fig. 3). This time interval was necessary since, as observed, the root mean square deviation determined by the GROMACS suite showed that a final conformation without profound topological changes occurred after 50 ns (fig. 3a and b). The root means square fluctuation (RMSF) calculated for the APN proteins showed that *T. licus licus* models exhibited similar flexibility compared with MsAPN1. Moreover, the predicted binding site motif (RXXFPXXDEP) (Nakanishi *et al.*, 2002) of all APNs was flanked by highly flexible regions (fig. 3c). For Cry toxins, the RMSF showed that flexibility was higher for domain II, loops 2 and 3 of Cry1Ab, whereas Cry1Ac showed greater flexibility in the N-acetylgalactosamine (GalNAc) binding region (fig. 3d).

After calculating the solvent accessibility surface for all models, it was found that the binding sites of the toxins were more exposed to the solvent over time, especially the Cry1Ac domain III GalNAc-binding region (fig. S3). For the APNs, the binding region between amino acids (MsAPN1: 133–175, TlAPN1: 135–177, TlAPN3: 142–182, TlAPN4: 127–170) increased their surface area to the solvent, while the conserved RXXFPXXDEP motif (MsAPN1: 175–196, TlAPN1: 178–198, TlAPN3: 183–203, TlAPN4: 171–191) exhibited no significant changes (fig. S3). Based on these analyses, the properties of Cry1Ac toxin suggest an interaction site that increases the toxin's affinity for the receptor and potentiates toxicity.

Docking of Cry1A toxins family with APNs

The protein docking studies were performed considering the APN models as the receptor protein and Cry1A family models as the

ligand proteins. MsAPN1 was experimentally described as a Cry1Aa (Nair and Dean, 2008), Cry1Ab (Pacheco *et al.*, 2009), and Cry1Ac (Cooper *et al.*, 1998) receptor and served here as a reference for the *in silico* study of Cry toxin binding to TlAPN1, TlAPN3, and TlAPN4 proteins (Fonseca *et al.*, 2015). Multiple sequence alignment of the APN-binding regions allowed mapping of amino acid residues involved in docking to the Cry1A toxins family. This analysis revealed that the interaction occurs at a common site preceding the RXXFPXXDEP region. In MsAPN1, the binding site was located in the region between Arg164 and Trp175, in TlAPN1 between Lys154 and Trp177, in TlAPN3 between Thr162 and Trp182, and in TlAPN4 in the region between Arg147 and Tyr170 (fig. S4).

Prior to protein docking, the MsAPN1-binding site was analyzed to determine which amino acid residues would be exposed at the surface (fig. S5). Using this information as a reference, we selected models in which the docking occurred with residues in regions accessible to the solvent: MsAPN1: Ile133–Pro196, TlAPN1: Ile135–Pro198, TlAPN3: Tyr142–Pro203, and TlAPN4: Ile127–Pro191. Considering the number of hydrogen bonds between the receptor-binding region and toxin domain II, loop 3, the Cry1Ac × MsAPN1 simulation revealed six likely interactions, followed by Cry1Ac × MsAPN1 with four interactions (table 2, fig. 4). The Cry1Aa × MsAPN1 simulation showed no hydrogen bonds with amino acids in domain II, loop 3 (table S1). The model with the most similar results for *T. licus licus* receptors and Cry toxins was the Cry1Ac × TlAPN4 combination with seven hydrogen bonds (table 2, fig. 5). The Cry1Ab × TlAPN4 simulation resulted in four hydrogen bonds between the receptor-binding site and toxin domain II, loop 3, whereas only one hydrogen bond was observed in the Cry1Aa × TlAPN4 simulation. The complete list of docking combinations and hydrogen bonds is shown in table S1. In summary, these *in silico* analyses allowed us to predict the putative interaction profile between Cry1A toxins and likely *T. licus licus* APN receptors.

Discussion

Cry protoxins are naturally proteolytically activated by the action of enzymes present in the alkaline gut homogenate. Proper
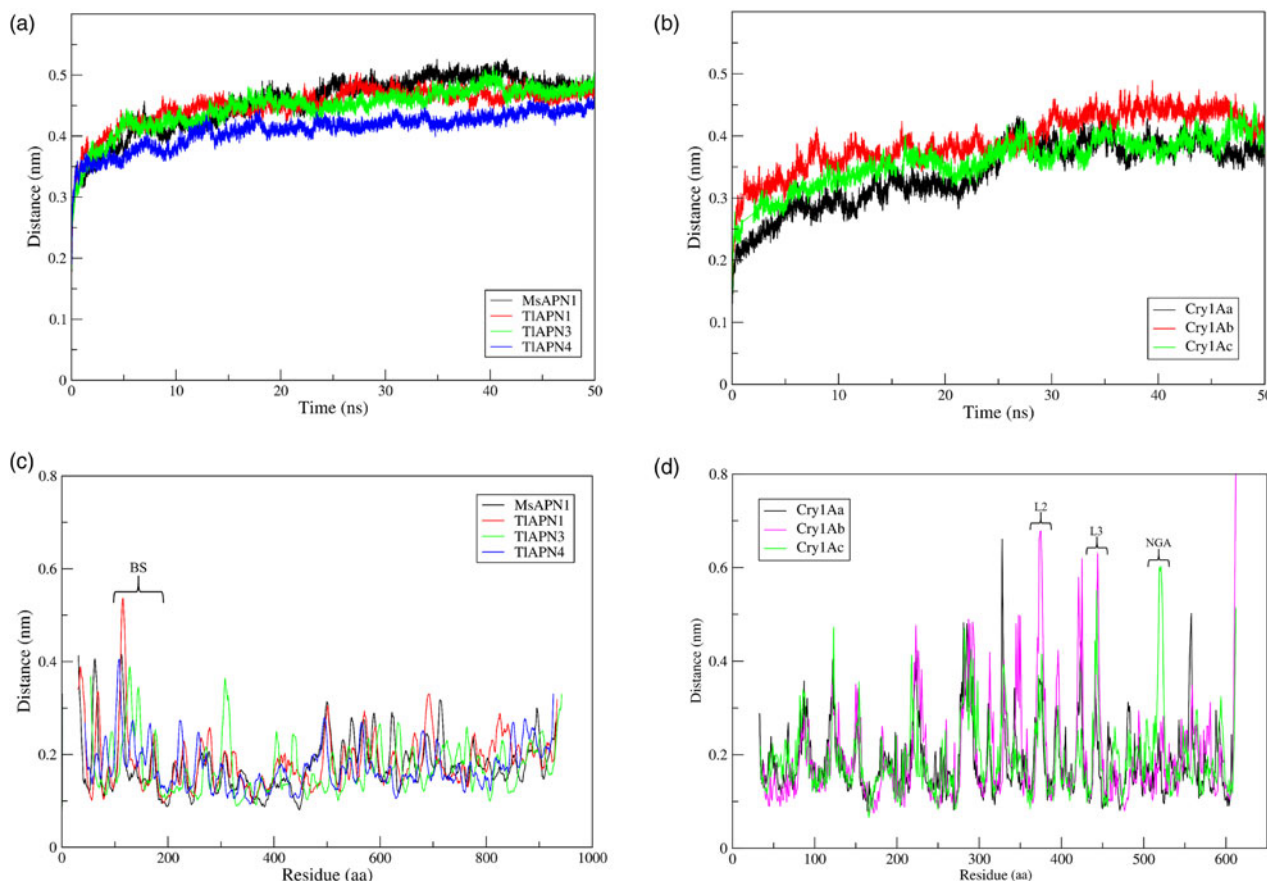
Figure 3. Molecular dynamics simulations of the APNs and Cry1A toxin family submitted to 50 ns. (a) Root mean square deviation (RMSD) of the topological changes of APN receptors after heating at 310 K. (b) RMSD of Cry1A toxin topological changes after heating at 310 K. (c) Root mean square fluctuation (RMSF) of APN receptor flexibility changes after heating at 310 K. (d) RMSF of Cry1A toxin flexibility changes of after heating at 310 K. BS, toxin-binding site; L2, toxin loop 2; L3, toxin loop 3; NGA, N-acetylgalactosamine-binding region.

activation limits the range of toxicity to insects with appropriate gut proteases (Aronson *et al.*, 1986; Talaei-Hassanloui *et al.*, 2014). Crystal solubilization and *in vitro* activation with commercial trypsin released two protein fragments for all the toxins. Upon incubation of these proteins with the intestinal homogenate of *T. licus licus*, the protoxins for all Cry1A toxins were cleaved into distinct fragments, whereas the Cry2Aa protein was almost completely digested. Lower mortality rates due to Cry2Aa could be occurred due to the lack of proper proteolytic activation or overdigestion of the toxin in the gut (Deist *et al.*, 2014). The same effect was observed following reduced trypsin activity, which resulted in increased resistance of *Plutella xylostella* larvae to Cry1Ac toxin (Gong *et al.*, 2020). Notably, screening tests with recombinant toxins applied to newborn *T. licus licus* larvae revealed that the Cry toxins evaluated in this study, Cry1A family and Cry2Aa, caused high mortality rates; however, Cry1Ac was the most active with the lowest median lethal concentration (LC$_{50}$), followed by Cry1Ab and Cry1Aa, whereas Cry2Aa required a higher concentration to produce the same effect.

An osmotic swelling assay was performed to determine the membrane disturbance ability of each recombinant toxin. The addition of trypsin-activated toxin increased the BBMVs turgor, as indicated by reduced light scattered, resulting in increased vesicle volume. The Cry1Ac, Cry1Ab, and Cry2Aa toxins caused more membrane disruption, followed by Cry1Aa, Cry1Ia12, and

Cry8Ka5. Similar effects have been observed previously (Soberón *et al.*, 2000; Kirouac *et al.*, 2006; Muñoz-Garay *et al.*, 2006; Groulx *et al.*, 2011), indicating that toxins from the Cry1A and Cry2A families are more effective against lepidopterans than the coleopteran-specific Cry8Ka5 (Oliveira *et al.*, 2011). Taking both analyses together, the observed differences in membrane disturbance and lethal activity between Cry1Aa and Cry2Aa could be due to crystal dissolution and activation in the insect midgut.

As a strategy to understand potential interactions between Cry toxins and *T. licus licus*, we employed bioinformatics tools and built structural models to identify Cry1A and TlAPN receptors. Using the *in silico* data, we were able to predict which proteins might act as the best Cry toxin receptors and suggest the amino acid residues that might interact between potential *T. licus licus* receptors and the toxins.

According to the pore formation mechanism, the first step is the interaction of domain II, loop 3 of a monomeric Cry1A toxin with an APN or an alkaline phosphatase located in the midgut epithelial cells. Domain II, loop 2 of the toxin, is usually related with binding to APN in the oligomeric structure (Gómez *et al.*, 2006; Pacheco *et al.*, 2009; Arenas *et al.*, 2010). In addition, Cry1Ac also binds through the β-16 strand region of domain III, which resembles a lectin, a protein that binds to carbohydrates such as GalNAc (de Maagd *et al.*, 1999). The

Table 2. Amino acid interactions observed between Cry1Ac toxins and APNs from *T. licus licus* (T1APN4) and *M. sexta* (MsAPN1)

	Cry1Ac × MsAPN1				Cry1Ac × TlAPN4			
	Toxin		Receptor		Toxin		Receptor	
Bond number	Atom	Residue	Atom	Residue	Atom	Residue	Atom	Residue
1	NH2	R249	O	V64	ND2	**N340**	O	S27
2	ND2	**N410**	OH	**Y167**	N	**N340**	OE1	E28
3	O	G307	NH1	**R170**	ND2	**N340**	OE1	E28
4	O	**G407**	N	**K173**	O	**P338**	NH1	**R110**
5	OD1	**N410**	NE	**R174**	O	**P338**	NH2	**R110**
6	OD1	**N410**	NH2	**R174**	NH2	R249	O	**I111**
7	O	**S411**	NH2	**R174**	NH1	R249	OE1	**E113**
8	ND2	**N410**	O	**W175**	NH2	R249	OE1	**E113**
9	NH2	R249	OE2	E209	OG	**S414**	OE1	**E113**
10	NH1	R279	OD2	D211	OG	**S411**	OE2	**E113**
11	O	**N410**	OG	S213	N	**V413**	OE2	**E113**
12	OD1	N311	NE2	N255	N	**S414**	OE2	**E113**
13	OG1	T302	O	G753	OG	**S411**	OH	**Y121**
14	OG	S261	O	A774	N	**S412**	OH	**Y121**
15	OH	Y306	OH	Y779	OG	**S412**	OH	**Y121**
16					O	**I341**	NZ	**K122**
17					O	**G342**	NZ	**K122**
18					NE2	**Q346**	OH	**Y124**
19					NH2	R279	O	**D129**
20					ND2	**N344**	OE1	**E130**
21					O	**I343**	OH	**Y133**
22					O	G307	ND1	H769
23					NH1	R417	OD2	D772
24					N	M309	OE1	Q773
25					ND2	**N410**	O	M775
26					OG	**S406**	OH	Y776
27					O	I416	OH	Y776
28					N	A418	OH	Y776
29					OG	**S412**	ND2	N777
30					NE2	**Q346**	OD2	D778
31					OD2	D276	NZ	K779
32					OH	Y283	NZ	K779
33					OG1	T308	NZ	K779
34					O	M309	NZ	K779
35					N	S409	OH	Y782
36					O	**N410**	OH	Y782
37					NH2	R405	O	Q808
38					O	I255	ND2	N809
39					OE1	E256	ND2	N809
40					OE1	E256	N	F810

(*Continued*)

Table 2. (*Continued.*)

Bond number	Cry1Ac × MsAPN1				Cry1Ac × TlAPN4			
	Toxin		Receptor		Toxin		Receptor	
	Atom	Residue	Atom	Residue	Atom	Residue	Atom	Residue
41					NE2	Q253	O	E812
42					O	S251	ND2	N816
43					OE1	Q253	OH	Y817

In bold underlined and orange, the amino acids in loops 2 and 3 of the toxin, respectively. In red and magenta, the amino acid region of the APN-binding site.

binding site of Cry1A toxins in the APN receptor has been identified as a region in domain I. As proposed by Nakanishi *et al.* (2002), for *Bombyx mori* APN1 (GenBank: AF084257), the region between residues Ile135–Pro198 has several conserved amino acids among different insect species; therefore, the authors suggested the RXXFPXXDEP motif as the most likely binding region. By analyzing the proposed region in the three-dimensional structure of APNs, we found that most RXXFPXXDEP residues are protected within the molecule and that a large conformational change would be required to allow access to the toxins, which was not observed in any structure after simulation and molecular docking. Sequence alignment of lepidopteran APNs demonstrated that the Cry1A toxin interaction region precedes the RXXFPXXDEP site and corresponds to the region observed in modeling with high flexibility. Here in the three-dimensional model of APNs, this region is formed by a loop and does not appear to depend on amino acid sequence conservation, as TlAPN3 and TlAPN4 have highly variable residue composition.

In this study, comparing the median lethal concentration (LC_{50}) data with the profile of the interactions formed between the monomeric toxins and the putative receptor in the molecular docking assays, a direct correlation was observed between toxicity and the total number of hydrogen bonds formed between the receptor-binding region and the toxin domain II, loop 3. The Cry1Ac × MsAPN1 interaction was the combination with the highest number of hydrogen bonds, followed by Cry1Ab × MsAPN1 and the Cry1Aa × MsAPN1 combination, which had no hydrogen bonds with domain II, loop3, but exhibited nine hydrogen bonds with domain II, loop 2. Different research groups have calculated the LC_{50} of Cry1A toxins against *M. sexta* larvae, and in general there are no significant differences between them. According to Carmona *et al.* (2011), the LC_{50} of Cry1Aa was 3.7 ng cm^{-2} (with a confidence interval (CI) of 2.8–4.7 ng cm^{-2}). For Cry1Ab, an LC_{50} of 2.9 ng cm^{-2} was observed (with a CI of 1.8–4.8 ng cm^{-2}). The calculated LC_{50} for Cry1Ac was 1.8 ng cm^{-2} (with a CI of 2.0–3.6 ng cm^{-2}). Although there was
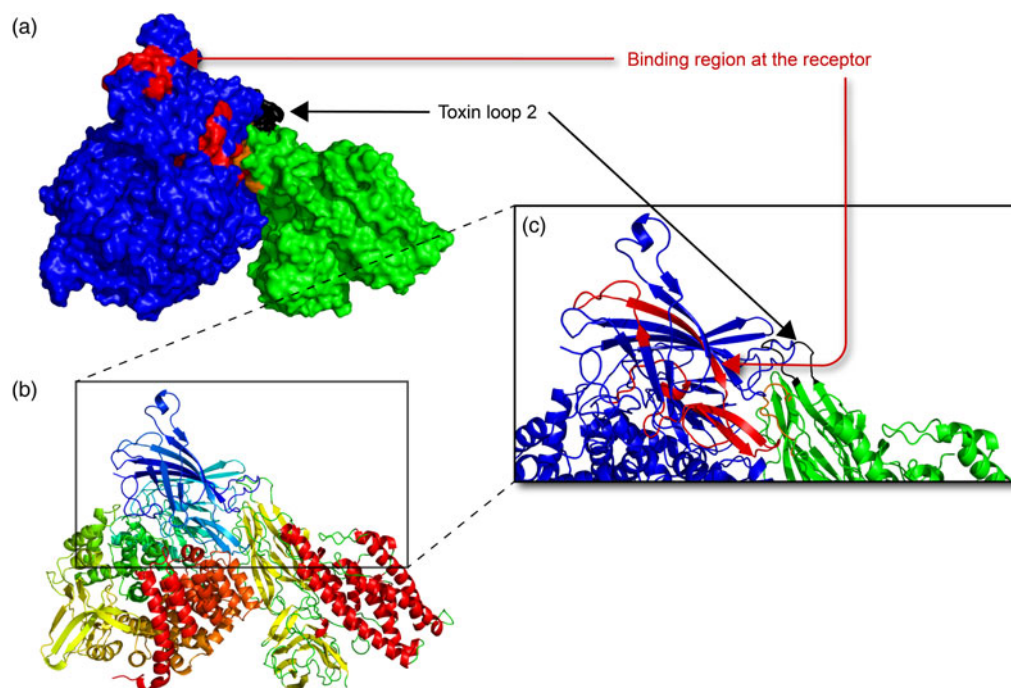
Figure 4. Schematic molecular docking representation of Cry1Ac binding to MsAPN1. (a) Surface representation of the interaction (MsAPN1 in blue and Cry1Ac in green). (b) Ribbon representation of the interaction (MsAPN1 on the left and Cry1Ac on the right). (c) Approximate view of the interaction (MsAPN1 in blue and Cry1Ac in green). In (a) and (c), red indicates the receptor-binding region, black indicates toxin loop 2, and orange indicates toxin loop.
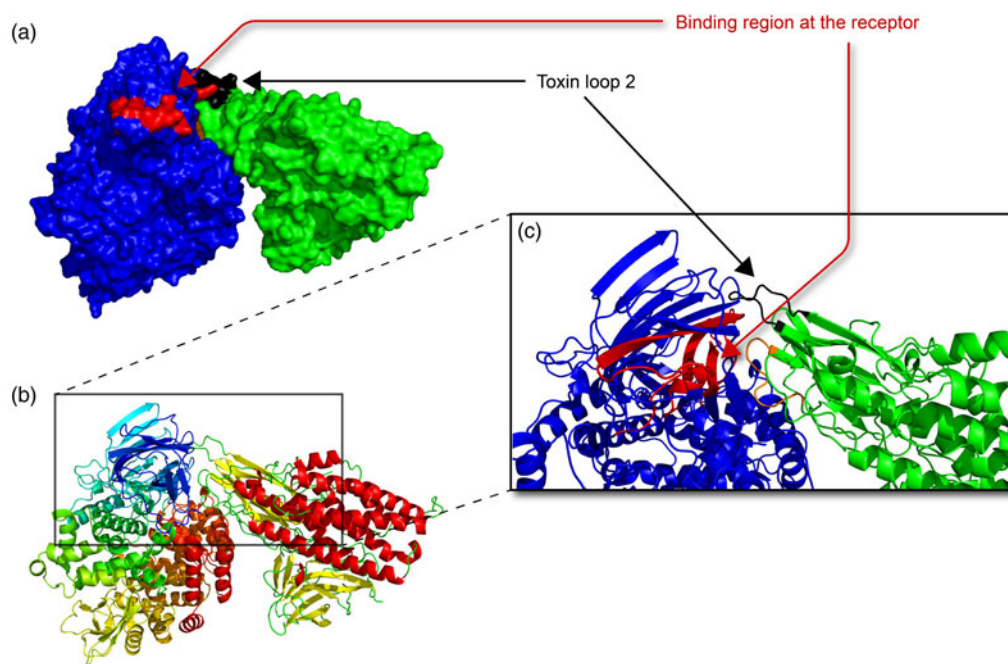
Figure 5. Schematic molecular docking representation of the Cry1Ac binding to TlAPN4. (a) Surface representation of the interaction (TlAPN4 in blue and Cry1Ac in green). (b) Ribbon representation of the interaction (Cry1Ac on the left and TlAPN4 on the right). (c) Approximate view of the interaction (TlAPN4 in blue and Cry1Ac in green). In (a) and (c), red indicates the receptor-binding region, black indicates toxin loop 2, and orange indicates toxin loop 3.

no significant difference in toxicity against *M. sexta*, Cry1Ac generally has lower LC_{50} values, followed by Cry1Ab and Cry1Aa. Taken together, these data suggest that the number of hydrogen bonds may increase the strength of the interaction, resulting in MsAPN1 preferentially binding to Cry1Ac.

Since the number of hydrogen bonds is known to play an important role in binding affinity in protein–protein interactions (Chen *et al.*, 2015; Javaid *et al.*, 2018), including for Cry toxins and their receptors (Tajne *et al.*, 2013; Florez *et al.*, 2018), we investigated the number of hydrogen bonds formed between Cry1A toxin and TlAPN receptors. Notably, Cry1Ac × TlAPN4 was identified as the protein combination that showed a similar pattern to that observed by the Cry1Ac × MsAPN1 assay. A total of 52 hydrogen bonds were formed, including seven interactions between receptor binding site residues and the toxin loop 3. Considering the number of hydrogen bonds formed between the toxins and TlAPN4, a direct correlation can be assumed with the toxicity observed in the bioassays. For instance, the LC_{50} calculated in the *T. licus licus* bioassay shows that although there were no significant differences between the activities of the Cry1A toxins, Cry1Ac tended to have lower LC50 values, followed by Cry1Ab and Cry1Aa. Although Cry1Ac toxicity depends on the number of hydrogen bonds formed with APN receptors, this toxin is known to interact with APN receptors through two distinct sites (Masson *et al.*, 1995; de Maagd *et al.*, 1999) and that domain III binding to GalNAc determines specificity and toxicity (de Maagd *et al.*, 1999). Additionally, Cry1Ac has been shown to interact with APN through the C-terminal region of the receptor (Yaoi *et al.*, 1999), which interrupts the pore formation process when removed from the protein sequence (Zhang *et al.*, 2009). The APN C-terminal region is thought to be filled with numerous O-glycosylations, mainly GalNAc, and it is suggested that the Cry1Ac domain III binds to one of these sugars (Stephens

et al., 2004). Examination of the likely O-glycosylated MsAPN1 residues reveals that at least two are located near the Ile135–Pro198 region, one of which is present in the C-terminal region. It was previously shown that glycosylations of *T. licus licus* APNs have a similar pattern to MsAPN1 and likely exert the same influence on Cry1Ac activity. Although weaker, loop 3 of Cry1Ac domain II can drive the interaction into a conformation in which it binds to APN domain I, and Cry1Ac domain III binds to GalNAcs present in APN domain IV. In this way, the interacting amino acid residues predicted for Cry1Ac in this work are likely those shared by the other Cry1A toxins and occur in the same region of APNs.

However, it should be noted that these data do not exclude the possibility that TlAPN1 and TlAPN3 may act as potential receptors of Cry toxins, which would need to be confirmed by further studies. The Cry1Ab × TlAPN1 interaction model suggests a very similar profile to that which occurred in *M. sexta*, with more hydrogen bonding than Cry1Ac × TlAPN4. The same pattern was observed for the interaction between Cry1Ab and TlAPN3, but with fewer hydrogen bonds. Most studies show that Cry1A toxins preferentially bind to APN1 (Zhang *et al.*, 2009; Yang *et al.*, 2010; Tiewsiri and Wang, 2011; Coates *et al.*, 2013; Qiu *et al.*, 2017), but it has also been shown that other APNs could act as toxin receptors. Although Cry1Aa and Cry1Ab could not bind to BBMVs of *B. mori* and *P. xylostella*, these toxins were able to bind to recombinant APN1–4 proteins (Nakanishi *et al.*, 2002). Furthermore, *Diatraea saccharalis* APN1–3 RNA silencing was found to be involved in reducing insect susceptibility to Cry1Ab (Yang *et al.*, 2010), while Cry1Ac interacted with *Helicoverpa armigera* APN2 (Rajagopal *et al.*, 2003). Thus, immediately after examining the expression level of each gene in conjunction with *in vitro* binding assays and identifying receptors other than APNs, the actual participation of each element in the mechanism of action will be known.

This study reported the noteworthy efficacy of four *Bt* Cry toxins toward sugarcane giant borer. We highlighted that the tested toxins caused high mortality of *T. licus licus* larvae, emphasizing the efficacy of Cry1Ac toxin. Furthermore, the *T. licus licus* transcripts database was used to gain insight into the binding interaction between Cry toxins and putative APN receptor combinations. *In silico* analyses allow us to suggest toxin receptors without resorting to labor-intensive protein–protein interaction screening and provide a novel, in-depth application of transcriptome data. Indeed, the new data highlighted here should be considered for prospecting suitable Cry toxin-based formulations with high toxicity against *T. licus licus*, as well as in the further development of transgenic crops resistant to this very serious insect pest of sugarcane fields.

References

Abbott WS (1925) A method of computing the effectiveness of an insecticide. *Journal of Economic Entomology* **18**, 265–267.

Arenas I, Bravo A, Soberón M and Gómez I (2010) Role of alkaline phosphatase from *Manduca sexta* in the mechanism of action of *Bacillus thuringiensis* Cry1Ab toxin. *Journal of Biological Chemistry* **285**, 12497–12503.

Aronson AI, Beckman W and Dunn P (1986) *Bacillus thuringiensis* and related insect pathogens. *Microbiological Reviews* **50**, 1–24.

Baranek J, Pogodziński B, Szipluk N and Zielezinski A (2020) TOXiTAXi: a web resource for toxicity of *Bacillus thuringiensis* protein compositions towards species of various taxonomic groups. *Scientific Reports* **10**, 1–12.

Berendsen HJC, Grigera JR and Straatsma TP (1987) The missing term in effective pair potentials. *The Journal of Physical Chemistry A* **91**, 6269–6271.

Berendsen HJC, van der Spoel D and van Drunen R (1995) GROMACS: a message-passing parallel molecular dynamics implementation. *Computer Physics Communications* **91**, 43–56.

Bradford MM (1976) A rapid and sensitive method for the quantitation of microgram quantities of protein utilizing the principle of protein-dye binding. *Analytical Biochemistry* **72**, 248–254.

Briseno SHR (2008) *Informações sobre: lepidopteros da família Castniidae – Distribuição geográfica das espécies conhecidas na américa tropical e subtropical e importância econômica da* Castnia licus Drury, 1773 *no nordeste do Brasil.* Maceió, AL: Cooperativa regional dos produtores de açúcar e álcool de Alagoas.

Carmona D, Rodríguez-Almazán C, Muñoz-Garay C, Portugal L, Pérez C, de Maagd RA, Bakker P, Soberón M and Bravo A (2011) Dominant negative phenotype of *Bacillus thuringiensis* Cry1Ab, Cry11Aa and Cry4Ba mutants suggest hetero-oligomer formation among different Cry toxins. *PLoS ONE* **6**(5), e19952. doi: 10.1371/journal.pone.0019952

Carroll J and Ellar DJ (1993) An analysis of *Bacillus thuringiensis* d-endotoxin action on insect-midgut-membrane permeability using a light-scattering assay. *European Journal of Biochemistry* **214**, 771–778. doi: 10.1111/j.1432-1033.1993.tb17979.x

Chen W, Liu C, Xiao Y, Zhang D, Zhang Y, Li X, Tabashnik BE and Wu K (2015) A toxin-binding alkaline phosphatase fragment synergizes Bt toxin Cry1Ac against susceptible and resistant *Helicoverpa armigera*. *PLoS ONE* **10**, 1–19.

Christou P, Capell T, Kohli A, Gatehouse JA and Gatehouse AMR (2006) Recent developments and future prospects in insect pest control in transgenic crops. *Trends in Plant Science* **11**, 302–308.

Coates BS, Sumerford DV, Siegfried BD, Hellmich RL and Abel CA (2013) Unlinked genetic loci control the reduced transcription of aminopeptidase N 1 and 3 in the European corn borer and determine tolerance to *Bacillus thuringiensis* Cry1Ab toxin. *Insect Biochemistry and Molecular Biology* **43**, 1152–1160.

Comeau SR, Gatchell DW, Vajda S and Camacho CJ (2004) ClusPro: a fully automated algorithm for protein-protein docking. *Nucleic Acids Research* **32** (Web Server issue), W96–9. doi: 10.1093/nar/gkh354

Cooper MA, Carroll J, Travis ER, Williams DH and Ellar DJ (1998) *Bacillus thuringiensis* Cry1Ac toxin interaction with *Manduca sexta* aminopeptidase N in a model membrane environment. *Biochemical Journal* **333**, 677–683.

Craveiro KIC, Júnior JEG, Silva MCM, Macedo LLP, Lucena WA, Silva MS, Júnior JDAdS, Oliveira GR, de Magalhães MTQ, Santiago AD and Grossi-de-Sa MF (2010) Variant Cry1Ia toxins generated by DNA shuffling are active against sugarcane giant borer. *Journal of Biotechnology* **145**, 215–221.

Crickmore N (2022) *Bacillus thuringiensis*. Toxin Nomenclature. In: Full list of delta-endotoxins. Available at http://www.lifesci.sussex.ac.uk/home/Neil_Crickmore/Bt (accessed 22 April 2022).

de Groot BL and Grubmüller H (2001) Water permeation across biological membranes: mechanism and dynamics of Aquaporin-1 and GlpF. *Science* **294**, 2353–2357.

Deist BR, Rausch MA, Fernandez-Luna MT, Adang MJ and Bonning BC (2014) Bt toxin modification for enhanced efficacy. *Toxins* **6**, 3005–3027.

de Maagd RA, Bakker PL, Masson L, Adang MJ, Sangadala S, Stiekema W and Bosch D (1999) Domain III of the *Bacillus thuringiensis* delta-endotoxin Cry1Ac is involved in binding to *Manduca sexta* brush border membranes and to its purified aminopeptidase N. *Molecular Microbiology* **31**, 463–471.

Essmann U, Perera L, Berkowitz ML, Darden T, Lee H and Pedersen LG (1995) A smooth particle mesh Ewald method. *The Journal of Chemical Physics* **103**, 8577–8593.

Fiser AS and Sali AS (2003) Modeller: generation and refinement of homology-based protein structure models. *Methods in Enzymology* **374**, 461–491.

Florez AM, Suarez-Barrera MO, Morales GM, Rivera KV, Orduz S, Ochoa R, Guerra D and Muskus C (2018) Toxic activity, molecular modeling and docking simulations of *Bacillus thuringiensis* Cry11 toxin variants obtained via DNA shuffling. *Frontiers in Microbiology* **9**, 2461.

Fonseca FCdA, Firmino AAP, de Macedo LLP, Coelho RR, de Sousa Júnior JDA, Silva-Junior OB, Togawa RC, Pappas GJ, de Góis LAB, da Silva MCM and Grossi-de-Sá MF (2015) Sugarcane giant borer transcriptome analysis and identification of genes related to digestion. *PLoS ONE* **10**, e0123836.

Fortier M, Vachon V, Kirouac M, Schwartz JL and Laprade R (2005) Differential effects of ionic strength, divalent cations and pH on the pore-

forming activity of *Bacillus thuringiensis* insecticidal toxins. *Journal of Membrane Biology* **208**, 77–87.

Gómez I, Oltean DI, Gill SS, Bravo A and Soberón M (2001) Mapping the epitope in cadherin-like receptors involved in *Bacillus thuringiensis* Cry1A toxin interaction using phage display. *Journal of Biological Chemistry* **276**, 28906–28912.

Gómez I, Sánchez J, Miranda R, Bravo A and Soberón M (2002) Cadherin-like receptor binding facilitates proteolytic cleavage of helix alpha-1 in domain I and oligomer pre-pore formation of *Bacillus thuringiensis* Cry1Ab toxin. *FEBS Letters* **513**, 242–246.

Gómez I, Arenas I, Benitez I, Miranda-Ríos J, Becerril B, Grande R, Almagro JC, Bravo A and Soberón M (2006) Specific epitopes of domains II and III of *Bacillus thuringiensis* Cry1Ab toxin involved in the sequential interaction with cadherin and aminopeptidase-N receptors in *Manduca sexta*. *Journal of Biological Chemistry* **281**, 34032–34039.

Gong L, Kang S, Zhou J, Sun D, Guo L, Qin J, Zhu L, Bai Y, Ye F, Akami M, Wu Q, Wang S, Xu B, Yang Z, Bravo A, Soberón M, Guo Z, Wen L and Zhang Y (2020) Reduced expression of a novel midgut trypsin gene involved in protoxin activation correlates with Cry1ac resistance in a laboratory-selected strain of *Plutella xylostella* (L.). *Toxins* **12**, 1–15.

Grossi-de-Sa MF, Silva MCM, Fonseca FCDA, Macedo LLP, Lourenço IT and Freire ÉVSA (2013) *Aparato e método de criação de larvas de insetos em laboratório*. INPI BR10201303033112–0 patent.

Groulx N, McGuire H, Laprade R, Schwartz JL and Blunck R (2011) Single molecule fluorescence study of the *Bacillus thuringiensis* toxin Cry1Aa reveals tetramerization. *Journal of Biological Chemistry* **286**, 42274–42282.

Herrero S, González-Cabrera J, Tabashnik BE and Ferré J (2001) Shared binding sites in Lepidoptera for *Bacillus thuringiensis* Cry1Ja and Cry1A toxins. *Applied and Environmental Microbiology* **67**, 5729–5734.

Hess B, Bekker H, Berendsen HJC and Fraaije JGEM (1997) LINCS: a linear constraint solver for molecular simulations. *Journal of Computational Chemistry* **18**, 14631472.

ISAAA (2020) Global status of commercialized biotech/GM crops in 2019: biotech crops drive socio-economic development and sustainable environment in the new frontier. In ISAAA Brief No. 55 (ISAAA Brie). Ithaca, NY: ISAAA. Available at http://www.isaaa.org/resources/publications/briefs/54/executivesummary/pdf/B54-ExecSum-English.pdf (accessed 19 March 2022).

Javaid S, Naz S, Amin I, Jander G, Ul-Haq Z and Mansoor S (2018) Computational and biological characterization of fusion proteins of two insecticidal proteins for control of insect pests. *Scientific Reports* **8**, 1–11.

Kirouac M, Vachon V, Quievy D, Schwartz JL and Laprade R (2006) Protease inhibitors fail to prevent pore formation by the activated *Bacillus thuringiensis* toxin Cry1Aa in insect brush border membrane vesicles. *Applied and Environmental Microbiology* **72**, 506–515.

Laskowski R, Hutchinson E, Michie A, Wallace A, Jones M and Thornton J (1997) PDBsum: a web-based database of summaries and analyzes of all PDB structures. *Trends in Biochemical Sciences* **22**, 488–490.

Lucena WA, Pelegrini PB, Martins-de-Sa D, Fonseca FCA, Gomes JE, de Macedo LLP, da Silva MCM, Sampaio R and Grossi-de-Sa MF (2014) Molecular approaches to improve the insecticidal activity of *Bacillus thuringiensis* cry toxins. *Toxins* **6**, 2393–2423.

Masson L, Lu Y-J, Masza A, Brousseauj R and Adan MJ (1995) The CryIA (c) receptor purified from *Manduca sexta* displays multiple specificities. *Journal of Biological Chemistry* **270**, 20309–20315.

Mendonça AF, Viveiros AJA and Sampaio FF (1996) A broca gigante da cana-de-açúcar, *Castnia licus* Drury, 1770 (Lep.: Castniidae). In Mendonça AF (ed.), *Pragas da cana-de-Açúcar*. Maceió: Insetos & Cia, pp. 133–167.

Monnerat RG, Batista AC, de Medeiros PT, Martins ÉS, Melatti VM, Praça LB, Dumas VF, Morinaga C, Demo C, Gomes ACM, Falcão R, Siqueira CB, Silva-Werneck JO and Berry C (2007) Screening of Brazilian *Bacillus thuringiensis* isolates active against *Spodoptera frugiperda*, *Plutella xylostella* and *Anticarsia gemmatalis*. *Biological Control* **41**, 291–295.

Muñoz-Garay C, Sánchez J, Darszon A, de Maagd RA, Bakker P, Soberón M and Bravo A (2006) Permeability changes of *Manduca sexta* midgut brush border membranes induced by oligomeric structures of different Cry toxins. *Journal of Membrane Biology* **212**, 61–68.

Nair MS and Dean DH (2008) All domains of Cry1A toxins insert into insect brush border membranes. *Journal of Biological Chemistry* **283**, 26324–26331.

Nakanishi K, Yaoi K, Nagino Y, Hara H, Kitami M, Atsumi S, Miura N and Sato R (2002) Aminopeptidase N isoforms from the midgut of *Bombyx mori* and *Plutella xylostella* – their classification and the factors that determine their binding specificity to *Bacillus thuringiensis* Cry1A toxin. *FEBS Letters* **519**, 215–220.

Noriega DD, Arraes FBM, Antonino JD, Macedo LLP, Fonseca FCA, Togawa RC, Grynberg P, Silva MCM, Negrisoli AS and Grossi-de-Sa MF (2020) Transcriptome analysis and knockdown of the juvenile hormone esterase gene reveal abnormal feeding behavior in the sugarcane giant borer. *Frontiers in Physiology* **11**, 588450.

Oliveira GR, Silva MC, Lucena WA, Nakasu EY, Firmino AA, Beneventi MA, Souza DS, Gomes JE, da De Souza J, Rigden DJ, Ramos HB, Soccol CR and Grossi-De-Sa MF (2011) Improving Cry8Ka toxin activity towards the cotton boll weevil (*Anthonomus grandis*). *BMC Biotechnology* **11**, 85. doi: 10.1186/1472-6750-11-85

Oliveira RS, Oliveira-Neto OB, Moura HFN, de Macedo LLP, Arraes FBM, Lucena WA, Lourenço-Tessutti IT, Barbosa AAD, da Silva MCM and Grossi-de-Sa MF (2016) Transgenic cotton plants expressing cry1Ia12 toxin confer resistance to fall armyworm (*Spodoptera frugiperda*) and cotton boll weevil (*Anthonomus grandis*). *Frontiers in Plant Science* **7**, 1–11.

Pacheco S, Gómez I, Arenas I, Saab-Rincon G, Rodríguez-Almazán C, Gill SS, Bravo A and Soberón M (2009) Domain II loop 3 of *Bacillus thuringiensis* Cry1Ab toxin is involved in a 'Ping Pong' binding mechanism with *Manduca sexta* aminopeptidase-N and cadherin receptors. *Journal of Biological Chemistry* **284**, 32750–32757.

Pardo-López L, Soberón M and Bravo A (2013) *Bacillus thuringiensis* insecticidal three-domain Cry toxins: mode of action, insect resistance and consequences for crop protection. *FEMS Microbiology Reviews* **37**, 3–22.

Peña G, Miranda-Rios J, de La Riva G, Pardo-López L, Soberón M and Bravo A (2006) A *Bacillus thurigiensis* S-layer protein involved in toxicity against *Epilachna varivestis* (Coleoptera: Coccinellidae). *Applied and Environmental Microbiology* **72**, 353–360.

Pinto ADS, Garcia JF and Oliveira HND (2006) Manejo das principais pragas da cana-de-açúcar. In Segato SV (ed.), *Atualização em Produção de cana-de-Açúcar*. Piracicaba, SP: CP2, pp. 257–280.

Qiu L, Zhang B, Liu L, Ma W, Wang X, Lei C and Chen L (2017) Proteomic analysis of Cry2Aa-binding proteins and their receptor function in *Spodoptera exigua*. *Scientific Reports* **7**, 1–10.

Rajagopal R, Agrawal N, Selvapandiyan A, Sivakumar S, Ahmad S and Bhatnagar RK (2003) Recombinantly expressed isoenzymic aminopeptidases from *Helicoverpa armigera* (American cotton bollworm) midgut display differential interaction with closely related *Bacillus thuringiensis* insecticidal proteins. *Biochemical Journal* **370**, 971–978.

Ribeiro TP, Arraes FBM, Lourenço-Tessutti IT, Silva MS, Lisei-de-Sá ME, Lucena WA, Macedo LLP, Lima JN, Santos Amorim RM, Artico S, Alves-Ferreira M, Mattar Silva MC and Grossi-de-Sa MF (2017) Transgenic cotton expressing Cry10Aa toxin confers high resistance to the cotton boll weevil. *Plant Biotechnology Journal* **15**, 997–1009.

Ribeiro TP, Basso MF, de Carvalho MH, de Macedo LLP, da Silva DML, Lourenço-Tessutti IT, de Oliveira-Neto OB, de Campos-Pinto ER, Lucena WA, da Silva MCM, Tripode BMD, Abreu-Jardim TPF, Miranda JE, Alves-Ferreira M, Morgante CV and Grossi-de-Sa MF (2019) Stability and tissue-specific Cry10Aa overexpression improves cotton resistance to the cotton boll weevil. *Biotechnology Research and Innovation* **3**, 27–41.

Rodrigo-Simón A, Caccia S and Ferré J (2008) *Bacillus thuringiensis* Cry1Ac toxin-binding and pore-forming activity in brush border membrane vesicles prepared from anterior and posterior midgut regions of lepidopteran larvae. *Applied and Environmental Microbiology* **74**, 1710–1716.

Shen M and Sali A (2006) Statistical potential for assessment and prediction of protein structures. *Protein Science* **15**, 2507–2524.

Silva-Brandão KL, Almeida LC, Moraes SS and Cônsoli FL (2013) Using population genetic methods to identify the origin of an invasive population and to diagnose cryptic subspecies of *Telchin licus* (Lepidoptera: Castniidae). *Bulletin of Entomological Research* **103**, 89–97.

Soberón M, Pérez RV, Nuñez-Valdéz ME, Lorence A, Gómez I, Sánchez J and Bravo A (2000) Evidence for intermolecular interaction as a necessary step for pore-formation activity and toxicity of *Bacillus thuringiensis* Cry1Ab toxin. *FEMS Microbiology Letters* **191**, 221–225.

Stephens E, Sugars J, Maslen SL, Williams DH, Packman LC and Ellar DJ (2004) The N-linked oligosaccharides of aminopeptidase N from *Manduca sexta*: site localization and identification of novel N-glycan structures. *European Journal of Biochemistry* **271**, 4241–4258.

Tajne S, Sanam R, Gundla R, Gandhi NS, Mancera RL, Boddupally D, Vudem DR and Khareedu VR (2012) Molecular modeling of Bt Cry1Ac (DI-DII)-ASAL (*Allium sativum* lectin)-fusion protein and its interaction with aminopeptidase N (APN) receptor *of Manduca sexta*. *Journal of Molecular Graphics and Modelling* **33**, 61–76.

Tajne S, Boddupally D, Sadumpati V, Vudem DR and Khareedu VR (2013) Synthetic fusion-protein containing domains of Bt Cry1Ac and *Allium sativum* lectin (ASAL) conferred enhanced insecticidal activity against major lepidopteran pests. *Journal of Biotechnology* **171**, 71–75.

Talaei-Hassanloui R, Bakhshaei R, Hosseininaveh V and Khorramnezhad A (2014) Effect of midgut proteolytic activity on susceptibility of lepidopteran larvae to *Bacillus thuringiensis* subsp. Kurstaki. *Frontiers in Physiology* **4**, 1–6.

Tiewsiri K and Wang P (2011) Differential alteration of two aminopeptidases N associated with resistance to *Bacillus thuringiensis* toxin Cry1Ac in cabbage looper. *Proceedings of the National Academy of Sciences of the USA* **108**, 14037–14042.

Vachon V, Laprade R and Schwartz JL (2012) Current models of the mode of action of *Bacillus thuringiensis* insecticidal crystal proteins: a critical review. *Journal of Invertebrate Pathology* **111**, 1–12.

van Gunsteren WF (1996) *Biomolecular Simulation: GROMOS 96 Manual and User Guide*. Zürich: Biomos.

Wolfersberger M, Luethy P, Maurer A, Parenti P, Sacchi FV, Giordana B and Hanozett GM (1987) Preparation and partial characterization of amino acid transporting brush border membrane vesicles from the larval midgut of the cabbage butterfly (*Pieris brassicae*). *Comparative Biochemistry and Physiology* **86**, 301–308.

Yang Y, Zhu YC, Ottea J, Husseneder C, Rogers Leonard B, Abel C and Huang F (2010) Molecular characterization and RNA interference of three midgut aminopeptidase N isozymes from *Bacillus thuringiensis*-susceptible and -resistant strains of sugarcane borer, *Diatraea saccharalis*. *Insect Biochemistry and Molecular Biology* **40**, 592–603.

Yaoi K, Nakanishi K, Kadotani T, Imamura M, Koizumi N, Iwahana H and Sato R (1999) *Bacillus thuringiensis* Cry1Aa toxin-binding region of *Bombyx mori* aminopeptidase N. *FEBBS Letter* **463**, 221–224.

Zhang S, Cheng H, Gao Y, Wang G, Liang G and Wu K (2009) Mutation of an aminopeptidase N gene is associated with *Helicoverpa armigera* resistance to *Bacillus thuringiensis* Cry1Ac toxin. *Insect Biochemistry and Molecular Biology* **39**, 421–429.